spectra and Dr. Birendra Pramanik and Peter Bartner for helpful discussions concerning interpretation of mass spectral data. We also thank Trudi Pier for expert typing of the text.

Registry No. **1a**, 83880-70-0; **1b**, 83880-73-3; **1c**, 83880-71-1; **1d**, 83880-72-2; **1e**, 83880-75-5; **1f**, 83881-10-1; **1g**, 83880-97-1; **1h**, 83880-77-7; **1i**, 83880-78-8; **1j**, 83880-79-9; **1k**, 83880-80-2; **1l**, 83881-16-7; **1m**, 83881-13-4; **1n**, 83880-83-5; **2a**, 83897-05-6; **2b**, 109218-04-4; **2c**, 83919-23-7; **2d**, 83881-14-5; **2e**, 83881-02-1; **2f**, 83880-86-8; **2g**, 83880-93-7; **2h**, 109183-48-4; **2i**, 83881-15-6; **2j**, 109183-49-5; **2k**, 83880-81-3; **3a**, 2995-86-0; **3b**, 4772-08-1; **4a**, 83880-69-7; **4b**, 83881-17-8; **4c**, 83881-18-9; **4d**, 83881-19-0; **5a**, 83880-74-4; **5b**, 109218-05-5; **5c**, 109183-50-8; **5d**, 109183-51-9; **6a**, 83880-76-6; **7**, 3872-52-4; **8**, 109183-52-0; **9a**, 83880-61-9; **9b**, 83881-05-4; **9c**, 83880-62-0; **10a**, 83880-65-3; **10b**, 107742-73-4; **10c**, 83881-01-0; **11a**, 1526-72-3; **11b**, 83880-85-7; **12**, 83880-91-5; **13a**, 2884-51-7; **13b**, 109183-56-4; **14**, 2325-61-3; **16a**, 912-24-3; **16b**, 109183-53-1; **17**, 109183-54-2; **18a**, 98422-34-5; **18b**, 109183-55-3; **19a**, 125-10-0; **19b**, 94813-60-2; 2-furoyl chloride, 527-69-5; 3-furoyl chloride, 26214-65-3; 2-thenoyl chloride, 5271-67-0; butyryl chloride, 141-75-3; methoxyacetyl chloride, 38870-59-6; dexamethasone 21-acetate, 1177-87-3; 5-methyl-2-thenoyl chloride, 31555-59-6.

Structure-Activity Relationships in an Imidazole-Based Series of Thromboxane Synthase Inhibitors

Paul W. Manley,*† Nigel M. Allanson,† Robert F. G. Booth, Philip E. Buckle,† Edward J. Kuzniar, Nagin Lad, Steve M. F. Lai,† David O. Lunt, and David P. Tuffin

Departments of Biology and Medicinal Chemistry, Searle Research and Development, Division of G. D. Searle & Co. Ltd., High Wycombe, Buckinghamshire HP12 4HL, U.K. *Received July 29, 1986*

Analogues of 4-[[2-(1*H*-imidazol-1-yl)-1-[[(4-methoxyphenyl)methoxy]methyl]ethoxy]methyl]benzoic acid (**5m**) were prepared and evaluated as thromboxane synthase inhibitors. A series of esters of **5m** showed a parabolic relationship between lipophilicity and inhibition of TxB_2 generation in intact platelets, with activities up to 50 times greater than that of dazoxiben. However, on administration to rabbits the ethyl ester **5d** had a short duration of action, due to rapid metabolism and excretion via deesterification and β-glucuronidation. Attempts at replacing the carboxylate group with other potential pharmacophores were unsuccessful.

The prostaglandin endoperoxide PGH_2 and its metabolites thromboxane A_2 (TxA_2) and prostacyclin (PGI_2) have been implicated in a number of physiological processes.[1-5] Thus TxA_2, in addition to being a constrictor of vascular smooth muscle, is a potent inducer of shape change, aggregation, and secretion in blood platelets, thereby playing an important role in hemostasis, thrombosis, and vasospasm. TxA_2 is produced from PGH_2 by the enzyme thromboxane synthase predominantly located within the cellular membrane of blood platelets, whereas PGI_2, which in many respects antagonizes the actions of TxA_2 in being a potent vasodilator and antiaggregatory agent, is formed from PGH_2 by prostacyclin synthase located in vascular endothelial cells. Currently used antiaggregatory drugs such as aspirin and sulfinpyrazone inhibit the prostaglandin cyclooxygenase enzyme responsible for the production of the PGH_2 precursor, prostaglandin endoperoxide PGG_2, in both platelets and endothelial cells, thereby indirectly reducing both PGI_2 and TxA_2 levels. Clearly, a compound that specifically inhibits TxA_2 synthase, while leaving PGI_2 levels unaffected or even increased, may be of clinical benefit in a wide range of vasospastic diseases.[6]

Purified TxA_2 synthase is a P-450 hemoprotein,[7] and studies suggest that the heme thiolate group of the enzyme is responsible for the coordination of the 9-O atom of the endoperoxide bond of PGH_2, which results in its cleavage and rearrangement to the oxetane acetal TxA_2 (Scheme I). The structure of TxA_2 has recently been confirmed by chemical synthesis.[8] The majority of the known inhibitors of TxA_2 synthase possess a basic nitrogen heterocycle, which is usually imidazole or pyridine.[9-17] Representatives of this class of compounds, such as dazoxiben (**1**) and CGS 13080 (**2**), inhibit Fe-CO complexation of the enzyme, suggesting that they act, at least in part, through

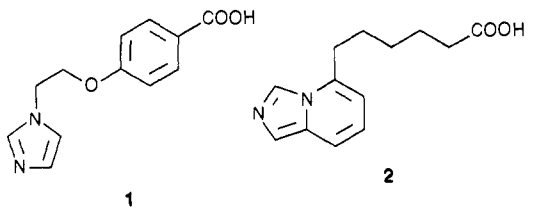

1 **2**

the nitrogen heterocycle displacing a 6-hydroxyl ligand from the heme and coordinating in its place to the Fe^{3+}

* Address for correspondence: Dr. P. W. Manley, Preclinical Research Department, Sandoz Ltd., CH-4002 Basel, Switzerland.
† Department of Medicinal Chemistry.

(1) Hamberg, M.; Svensson, J.; Samuelsson, B. *Proc. Natl. Acad. Sci. U.S.A.* **1975**, *72*, 2994.
(2) Moncada, S.; Gryglewski, R. J.; Bunting, S.; Vane, J. R. *Nature (London)* **1976**, *263*, 663.
(3) Gryglewski, R. J.; Bunting, S.; Moncada, S.; Flower, R. J.; Vane, J. R. *Prostaglandins* **1976**, *12*, 685.
(4) Moncada, S.; Gryglewski, R. J.; Bunting, S.; Vane, J. R. *Prostaglandins* **1976**, *12*, 715.
(5) Tada, M.; Kuzuya, T.; Inoue, M.; Kodama, K.; Mishima, M.; Yamada, M.; Inui, M.; Abe, H. *Circulation* **1981**, *64*, 1107.
(6) For a detailed discussion, consult: *Br. J. Clin. Pharmacol.* **1983**, *15* (Suppl. 1), 7-140S.
(7) Haurand, M.; Ullrich, V. *J. Biol. Chem.* **1985**, *260*, 15059.
(8) Bhagwat, S. S.; Hamann, P. R.; Still, W. C. *J. Am. Chem. Soc.* **1985**, *107*, 6372.
(9) Iizuka, K.; Akahane, K.; Momose, D.; Nakazawa, M.; Tanouchi, T.; Kawamura, M.; Ohyama, I.; Kajiwara, I.; Iguchi, Y.; Okada, T.; Taniguchi, K.; Miyamoto, T.; Hayashi, M. *J. Med. Chem.* **1981**, *24*, 1139.
(10) Tanouchi, T.; Kawamura, M.; Ohyama, I.; Kajiwara, I.; Iguchi, Y.; Okada, T.; Miyamoto, T.; Taniguchi, K.; Hayashi, M.; Iizuka, K.; Nakazawa, M. *J. Med. Chem.* **1981**, *24*, 1149.
(11) Gorman, R. R.; Johnson, R. A.; Spilman, C. H.; Aiken, J. W. *Prostaglandins* **1983**, *26*, 325.
(12) Ambler, J.; Butler, K. D.; Ku, E. C.; Maguire, E. D.; Smith, J. R.; Wallis, R. B. *Br. J. Pharmacol.* **1985**, *86*, 497.
(13) Kato, K.; Ohkawa, S.; Terao, S.; Terashita, Z.; Nishikawa, K. *J. Med. Chem.* **1985**, *28*, 287.
(14) Ford, N. F.; Browne, L. J.; Campbell, T.; Gemenden, C.; Goldstein, R.; Gude, C.; Wasley, J. W. F. *J. Med. Chem.* **1985**, *28*, 164.

0022-2623/87/1830-1588$01.50/0

Scheme I

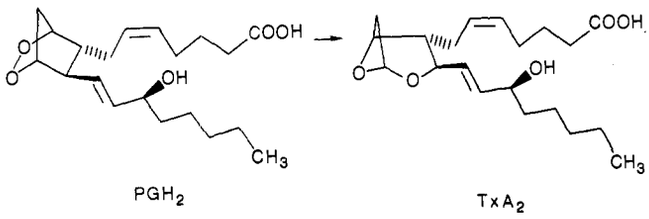

atom.[18] In addition to the heterocyclic group, many TxA_2 synthase inhibitors incorporate a carboxylic acid/acid derivative, separated from the basic N atom of the heterocycle by a distance of 8–10 Å. This distance corresponds approximately to that between the endoperoxide 9-O atom and the carboxylic acid group in PGH_2. Thus it appears likely that these TxA_2 synthase inhibitors primarily act by coordination of the heterocycle to the catalytic site of the enzyme, with the carboxylate group interacting with the PGH_2–COOH binding site.

In the course of our search for potential antithrombotic agents we identified SC 38249 (**5a**), a compound possessing significant antithrombotic activity, which was due in part to inhibition of TxA_2 synthase ($IC_{50} = 9.9 \times 10^{-6}$ M vs. human platelet TxB_2 generation). In an attempt to optimize this enzyme inhibitory activity, we initially investigated the incorporation of a carboxylate group into the molecule. In this paper the synthesis, in vitro structure–activity relationships, pharmacology, and metabolism of a series of imidazole-based TxA_2 synthase inhibitors arising out of this study are discussed.

Chemistry

The imidazole derivatives used in this study were all prepared as racemic mixtures according to Scheme II, with subsequent functional group manipulation of the ethers (**5**) where necessary. The synthesis of the intermediate imidazole ethanols (**4a** and **4b**) was accomplished by addition of imidazole to the oxiranes (**3a** and **3b**), which were readily available from the reaction of the sodium salt of the appropriate benzyl alcohol and epibromohydrin. Etherification of the alcohols (**4a** and **4b**) was generally achieved again by reacting the sodium alkoxide in THF with the appropriate benzylic halide, although **5a** was prepared in better yield by using KOH in Me_2SO.

Modifications to the carboxylate group of compound **5d** were made via saponification to the acid **5m**, followed by esterification (**5e,f**) or amidation (**5n–q**). The amide **5p** was readily converted to the corresponding thioamide **5r** by using Lawesson's reagent. Oxidation of the methylthio group of compound **5s** with either 1 or 2 equiv of *m*-chloroperoxybenzoic acid afforded the sulfoxide **5t** or sulfone **5u**, respectively.

The target compounds **5a–v** were generally either low-melting solids or hygroscopic gums, and, with the exception of **5t**, they were readily purified by flash column chromatography (silica gel) and characterized by high-field proton NMR spectroscopy and elemental analysis. Although no satisfactory elemental analysis could be obtained for the highly hygroscopic sulfoxide **5t**, it was adequately characterized from its IR, NMR, and mass spectral data and shown to be homogeneous by TLC and reversed-phase HPLC.

Scheme II.[a] Synthesis of Imidazole Derivatives

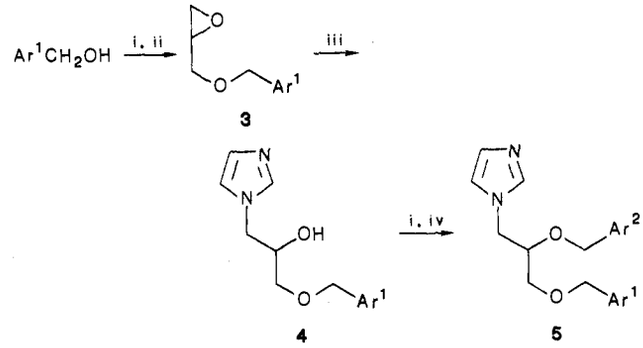

[a] Reagents: (i) NaH, THF; (ii) epibromohydrin; (iii) imidazole, THF; (iv) Ar^2CH_2Br.

Pharmacological Results and Discussion

Enzyme Inhibition. Enzyme activity was routinely measured in collagen-stimulated human platelets by radioimmunoassay of supernatant levels of TxB_2 (the stable metabolite of TxA_2). The inhibitory activities of the imidazole derivatives (**5a–v**) against intact human platelet TxA_2 formation, expressed as IC_{50} values, are shown in Table I. Furthermore, in the case of four compounds, inhibitory potency was determined against human platelet microsomal TxA_2 synthase activity measured directly by radioimmunoassay of TxB_2 produced from PGH_2 added as substrate (data included in Table I). Certain representative compounds from within the series were also evaluated for the selectivity of the inhibitory activity demonstrated against thromboxane formation with reference to other steps in the arachidonic acid pathway via cyclooxygenase. Firstly, to establish that these compounds possessed no inhibitory effect on the release of arachidonic acid from membrane phospholipid or its subsequent conversion to PGH_2, PGE_2 production in collagen stimulated human platelet rich plasma was measured by radioimmunoassay in the presence of **5d** and **5g** over a range of concentrations identical with those that inhibited TxB_2 generation. Rather than causing a reduction in plasma PGE_2 levels or leaving them unchanged, **5d** and **5g** (both 0.1–30.0 μM) induced a measurable increase in plasma PGE_2. The increase in PGE_2 levels observed was in both cases reproducible (duplicate experiments), significant ($p < 0.05$ vs. vehicle controls), and dose-related, occurred in parallel with inhibition of TxB_2 formation, and represented a >10-fold increase in PGE_2 present at the highest drug concentrations examined. These data strongly infer that the phospholipase A_2 and cyclooxygenase enzymes were not inhibited at the drug concentrations tested and, moreover, that progressive attenuation of thromboxane formation resulted in an increasing pool of PGH_2 available for other prostaglandin pathways. Secondly, compounds **5a** and **5d** were assessed for selectivity of inhibitory potency against TxA_2 synthase over PGI_2 synthase by evaluating their effect on PGI_2 synthesis in arachidonic acid stimulated, cultured bovine fetal heart endothelial cells in vitro. PGI_2 levels in the incubate were monitored by radioimmunoassay of its stable breakdown product 6-keto $PGF_{1\alpha}$ (as immunological equivalents). Compounds **5a** and **5d** were found to possess moderate inhibitory activity in this system, giving IC_{50} values of 51.0 μM and 17.7 μM, respectively (mean of three determinations), which represented a platelet TxA_2 synthase to vascular en-

(15) Cross, P. E.; Dickinson, R. P.; Parry, M. J.; Randall, M. J. *J. Med. Chem.* **1985**, *28*, 1427.
(16) Cross, P. E.; Dickinson, R. P.; Parry, M. J.; Randall, M. J. *J. Med. Chem.* **1986**, *29*, 342.
(17) Wright, W. B.; Press, J. B.; Chan, P. S.; Marsico, J. W.; Haug, M. F.; Lucas, J.; Tauber, J.; Tomcufcik, A. S. *J. Med. Chem.* **1986**, *29*, 523.
(18) Ullrich, V.; Haurand, M. *Adv. Prostaglandin, Thromboxane, Leukotriene Res.* **1983**, *11*, 105.

Table I. Physicochemical Data and Inhibitory Activity of Imidazole Derivatives vs. TxB_2 Generation in Intact Human Platelets and by Microsomal TxA_2 Synthase

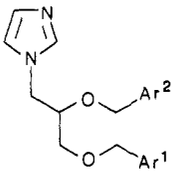

compd	Ar^1	Ar^2	method[a]	yield,[b] %	mp, °C	formula (anal.)[c]	IC_{50}[d] (μM) vs. human platelets	IC_{50}[d] (μM) vs. microsomal enzyme
5a	4-C_6H_4OMe	4-C_6H_4OMe	A	63	73–74[e]	$C_{22}H_{26}N_2O_4$ (C, H, N)	9.9 (±0.8)[k]	
5b	4-$C_6H_4CO_2Et$	4-C_6H_4OMe	A	33	54–55[f]	$C_{24}H_{28}N_2O_5 \cdot 0.5H_2O$ (C, H, N, H_2O)	3.6 (±1.2)	
5c	4-C_6H_4OMe	4-$C_6H_4CO_2Me$	A	27	77–78[g]	$C_{23}H_{26}N_2O_5$ (C, H, N)	1.26 (±0.82)	
5d	4-C_6H_4OMe	4-$C_6H_4CO_2Et$	A	28	58–59[h]	$C_{24}H_{28}N_2O_5$ (C, H, N)	0.54 (±0.07)	5.3
5e	4-C_6H_4OMe	4-$C_6H_4CO_2$-*n*-Pr	B	36	44–45[i]	$C_{25}H_{30}N_2O_5$ (C, H, N)	0.18 (±0.06)	
5f	4-C_6H_4OMe	4-$C_6H_4CO_2$-*i*-Pr	B	40	oil	$C_{25}H_{30}N_2O_5 \cdot 0.5H_2O$ (C, H, N, H_2O)	1.61 (±0.62)	
5g	4-C_6H_4OMe	4-$C_6H_4CO_2$-*n*-Bu	B	50	34–35[h]	$C_{26}H_{32}N_5O_5$ (C, H, N)	0.20 (±0.07)	2.0
5h	4-C_6H_4OMe	4-$C_6H_4CO_2Ph$	B	53	oil	$C_{28}H_{28}N_2O_5 \cdot 1.6H_2O$ (C, H, N, H_2O)	0.56 (±0.18)	
5i	4-C_6H_4OMe	4-$C_6H_4CO_2$-CH_2Ph	B	35	oil	$C_{29}H_{30}N_2O_5 \cdot 0.2H_2O$ (C, H, N, H_2O)	1.49 (±0.19)	7.1
5j	4-C_6H_4OMe	4-$C_6H_4CO_2$-*n*-C_8H_{17}	B	30	oil	$C_{30}H_{40}N_2O_5 \cdot 0.5H_2O$ (C, H, N, H_2O)	21.0 (±8.9)	
5k	4-C_6H_4OMe	3-$C_6H_4CO_2Et$	A	30	oil	$C_{24}H_{28}N_2O_5 \cdot 0.5H_2O$ (C, H, N, H_2O)	7.2 (±1.1)	
5l	4-C_6H_4OMe	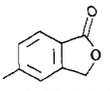	A	23	oil	$C_{23}H_{24}N_2O_5 \cdot 0.5H_2O$ (C, H, N, H_2O)	6.2 (±2.3)	
5m	4-C_6H_4OMe	4-$C_6H_4CO_2H$		80	109–111[h]	$C_{22}H_{24}N_2O_5$ (C, H, N)	6.7 (±1.7)	1.1
5n	4-C_6H_4OMe	4-$C_6H_4CONH_2$	B	51	oil	$C_{22}H_{25}N_3O_4 \cdot 0.8H_2O$ (C, H, N, H_2O)	6.0 (±2.8)	
5o	4-C_6H_4OMe	4-$C_6H_4CONHEt$	B	41	oil	$C_{24}H_{29}N_3O_4 \cdot 1.0H_2O$ (C, H, N, H_2O)	12.4 (±6.0)	
5p	4-C_6H_4OMe	4-$C_6H_4CONMe_2$	B	43	oil	$C_{24}H_{29}N_3O_4 \cdot 0.25H_2O$ (C, H, N, H_2O)	1.94 (±0.70)	
5q	4-C_6H_4OMe	4-C_6H_4CONMe-*n*-Bu	B	16	oil	$C_{27}H_{35}N_3O_4 \cdot 0.5H_2O$ (C, H, N, H_2O)	5.4 (±0.5)	
5r	4-C_6H_4OMe	4-$C_6H_4CSNMe_2$		48	oil	$C_{24}H_{29}N_3O_3S \cdot 0.6H_2O$ (C, H, N, S, H_2O)	12.4 (±3.0)	
5s	4-C_6H_4OMe	4-C_6H_4SMe	A	49	55–56[f]	$C_{22}H_{26}N_2O_3S$ (C, H, N, S)	6.4 (±1.9)	
5t	4-C_6H_4OMe	4-C_6H_4SOMe		25	oil	$C_{22}H_{26}N_2O_4S$[j]	8.6 (±3.6)	
5u	4-C_6H_4OMe	4-$C_6H_4SO_2Me$		71	72–74[h]	$C_{22}H_{26}N_2O_5S$ (C, H, N, S)	24.9 (±4.0)	
5v	4-$C_6H_4CO_2Et$	4-$C_6H_4CO_2Et$	A	39	49–50[f]	$C_{26}H_{30}N_2O_6$ (C, H, N)	0.70 (±0.10)	
dazoxiben							1.29 (±0.17)	

[a] Capital letters refer to synthetic methods A and B in the Experimental Section. [b] Yields were not optimized. [c] All compounds had C, H, and N analyses within ±0.40% of the theoretical values. [d] Molar concentration of test compound required to reduce the amount of TxB_2 (the stable metabolite of TxA_2) formed from PGH_2 by 50%. [e] Recrystallized from acetone–hexane. [f] Recrystallized from Et_2O–hexane. [g] Recrystallized from CH_2Cl_2–toluene. [h] Recrystallized from Et_2O–pentane. [i] Recrystallized from pentane. [j] No satisfactory elemental analysis could be obtained for this compound (see Experimental Section). [k] Mean (>3 determinations) ± SEM. [l] Mean (2 experiments) with all treatments in each experiment performed in duplicate.

dothelial cell PGI_2 synthase selectivity ratio (IC_{50} ratio) of 33 for compound **5d**.

Structure–Activity Relationships of Thromboxane Synthase Inhibition. The activities of the compounds reported in this study reveal some clear trends in the structure–activity requirements for the inhibition of TxA_2 synthase in human platelets. The effect of replacing either of the methoxy groups in **5a** with a ethoxycarbonyl group resulted in an increase in potency, although **5d** (Ar^2 = CO_2Et) was 7-fold more active than **5b** (Ar^1 = CO_2Et), suggesting that the effect was not simply due to an increase in the overall lipophilicity of the molecules, but to a discrete drug–receptor interaction. That there was a clear spatial requirement for the carboxylate group was confirmed by the observations that the meta ester **5k** was significantly less active than the para ester **5d** and that there was no additve or synergistic effect with the bis ester **5v**.

Despite the activity of dazoxiben (**1**) against TxB_2 formation in human platelets, **5m**, which like dazoxiben has a benzoic acid pharmacophore, was significantly less active than the corresponding ethyl ester **5d**. Consequently, in order to examine the effect of the carboxylate group on activity, we prepared a series of esters (**5c–j**) of differing hydrophobicity and size. The physicochemical parameters for hydrophobicity and bulk selected for this study were the site-specific descriptors *group hydrophobicity* (for COOR) and *group refractivity* (for R), and their values for **5m** and **5c–j** are shown in Table II.

The most active members of this set of compounds were the *n*-propyl and *n*-butyl analogues **5e** and **5g**. From regression analysis of the ester structure–activity data in Tables I and II, eq 1, 2 and 3 (Table III) were derived for group hydrophobicity (π) and group refractivity (R), respectively. Equations 1 and 3 clearly describe parabolic relationships between the pIC_{50}'s for the inhibition of human platelet TxB_2 formation and π and R. The similarity between these correlations may in part be due to the relationship between hydrophobicity and refractivity, which is often found in a homologous series of hydrophobic compounds having constant electronic properties and similar basic geometry, and is described here for the compounds in Table II by eq 4. The correlation between pIC_{50} and refractivity described by eq 3 was strong (r = 0.917), with the only major outlier being the bulky isopropyl ester **5f**, which was substantially less active than calculated (residual = −0.64). Furthermore, on the basis of their hydrophobicity, the bulky esters **5f**, **5h**, and **5i** were all less active than predicted by eq 1, and reanalysis of the data, giving only a 10% weight to these compounds, resulted in

Table II. Physical Parameters and SAR Data for Imidazole Ester Derivatives

compd	group hydrophobicity for COOR	group refractivity for R[a]	pIC_{50} obsd[b]	pIC_{50} (eq 2) calcd[c]	pIC_{50} (eq 2) error	pIC_{50} (eq 3) calcd[d]	pIC_{50} (eq 3) error
5m	−0.32[e]	1.68	5.1739	5.3045	−0.1306	5.2053	−0.0314
5c	−0.01[e]	6.34	5.8996	5.7387	0.1610	5.8035	0.0962
5d	0.51[e]	11.0	6.2676	6.2831	−0.0155	6.2128	0.0548
5e	1.03[f]	15.66	6.7447	6.5973	0.1474	6.4333	0.3114
5f	0.90[f]	15.66	5.7932	6.5404	−0.7472	6.4333	−0.6401
5g	1.55[f]	20.32	6.6990	6.6813	0.0176	6.4650	0.2340
5h	1.46[g]	25.36	6.2518	6.6833	−0.4314	6.2867	−0.0349
5i	1.84[h]	31.32	5.8268	6.6282	−0.8013	5.7909	0.0359
5j	3.66[f]	38.96	4.6778	4.6597	0.0181	4.7036	−0.0258

[a] Data taken from ref 19. [b] Experimental value from Table I. [c] Calculated from eq 2, Table III. [d] Calculated from eq 3, Table III. [e] Data taken from ref 20. [f] Calculated from $\pi_{COOEt} + \Sigma f_{CH}$ by the method of R. F. Rekker in ref 21. [g] Data taken from ref 22. [h] Calculated from $\pi_{COOMe} - f_H + f_{C_6H_5}$ by the method of R. F. Rekker in ref 21.

Table III. Correlation Equations Derived from Regression Analysis for the Inhibition of TxA_2 Synthase in Intact Platelets by Imidazole Ester Derivatives

correlation equation[a]	n[b]	r[c]	s[d]	eq no.
$pIC_{50} = 5.7175\ (\pm 0.2126) + 0.9071\ (\pm 0.2900)\pi - 0.3294\ (\pm 0.0809)\pi^2$	9	0.871	0.382	1
$pIC_{50} = 5.7513\ (\pm 0.1041) + 1.2599\ (\pm 0.1666)\pi - 0.4257\ (\pm 0.0459)\pi^2$	9[e]	0.971	0.220	2
$pIC_{50} = 4.9434\ (\pm 0.2994) + 0.1632\ (\pm 0.0335)R - 0.004\,35\ (\pm 0.000\,80)R^2$	9	0.917	0.310	3
$\pi = 0.094\,80\ (\pm 0.010\,05)R - 0.5717\ (\pm 0.2173)$	9	0.963	0.339	4

[a] $pIC_{50} = -\log IC_{50}$; π = group hydrophobicity; R = group refractivity. [b] Number of data points used in regression. [c] Correlation coefficient. [d] Standard deviation from regression line. [e] Includes 10% weighting to compounds **5f**, **5h**, and **5i**.

eq 2 in which the correlation ($r = 0.971$) was much improved over that for eq 1 ($r = 0.871$). These initial findings could be interpreted as being consistent with a hydrophobic interaction between the ester group and the enzyme, in which there are certain limitations regarding the bulk (as indicated by the anomalous behavior of **5f**, **5h**, and **5i**) and the size of the ester group (indicated by the inactivity of **5j**).

However, when representative compounds were tested against microsomal TxA_2 synthase (Table I), these structure–activity relationships broke down, with the acid **5m** now being the most potent compound. This latter finding infers that the parent acid, **5m**, is the active species and that its relative inactivity against TxB_2 generation in intact human platelets may be a result of the compound being ionized under the conditions of the assay, leading to increased hydrophilicity, and consequently having an adverse effect on the ability of the compound to permeate the platelet membrane. The structure–activity trends observed for the esters are then consistent with the more hydrophobic compounds most readily crossing the platelet membrane prior to being subjected to enzymatic hydrolysis to the active acid, **5m**, and interacting with the TxA_2 synthase located inside the platelet. The drop in activity observed for esters having group hydrophobicities greater than 1.5 may be ascribed to these more bulky compounds being poorer substrates for the esterase. Additional support for this hypothesis comes from the decrease in activity observed for **5l**, which has similar physicochemical parameters to **5c** and **5d** but due to its lactone structure is predicted to be more resistant to esterase hydrolysis.

In view of the above findings, we investigated the effect of replacing the carboxylate group with other potential pharmacophores. Our initial approach of incorporating polar carboxamide groups identified the tertiary amide **5p** as having comparable activity to dazoxiben, whereas the less hydrophobic primary and secondary amides with their capacity to act as hydrogen-bond donors were less active. In contrast to the esters, an increase in the hydrophobicity of the tertiary amide, as in **5q**, resulted in no improvement in TxA_2 synthase inhibition in human platelets.

In order to test the importance of the amide carbonyl group, we examined the thioamide **5r** and found it to be significantly less active than its oxo equivalent, **5p**. In view of the weak hydrogen-bond-acceptor properties of thioamides with respect to amides (pK_B for $CSNR_2 = 1.6$, pK_B for $CONR_2 = 2.76$, in which pK_B represents the logarithm of the ability of the group to accept a proton from 4-nitrophenol in CH_3CCl_3[23]), this result suggests that the amide carbonyl group could be acting as a hydrogen bond acceptor. In addition, compound **5t**, incorporating the potent hydrogen-bond-accepting sulfoxide functionality (pK_B for ArSOR = 2.7), despite being strongly hydrophilic (group hydrophobicity for $SOCH_3 = -1.35$) and therefore having a relatively poor platelet permeability, was weakly active. Furthermore, **5t** was more active than the corresponding sulfone **5u** (pK_B for $ArSO_2R = 1.6$, group hydrophobicity for $SO_2CH_3 = -1.28$), again pointing to a possible hydrogen-bond-acceptor contribution to the drug–enzyme binding energy.

Effect on Collagen-Induced Rabbit Whole Blood Thromboxane B_2 Formation ex Vivo. The effect of compound **5d** on collagen-induced TxB_2 formation in rabbit citrated whole blood ex vivo was determined following intravenous or oral dosing. Intravenous administration of **5d** (10 mg kg^{-1}) as a bolus injection in acidified saline (pH 6.0) resulted in an initial peak inhibitory effect (0.5 h after dosing) of 72 ± 10% ($p < 0.02$ vs. vehicle; $n = 5$), which declined rapidly at subsequent time points of 1 and 2 h, such that by 3 and 6 h, no significant inhibitory activity was evident (Figure 1). When administered orally, the compound inhibited collagen-induced TxB_2 formation ex vivo at 1 and 2 h after a 100 mg kg^{-1} dose (formulated in 10% polyethylene glycol–90% (carboxymethyl)cellulose (v/v)) compared to animals given vehicle alone (Figure 2); however, no significant activity was observed at lower doses of 30 and 10 mg kg^{-1} (data not shown). Thus, the activity of the compound in this test system declined rapidly

(19) Craig, P. N. *J. Med. Chem.* **1971**, *14*, 680.
(20) Hansch, C.; Leo, A.; Unger, S. H.; Kim, K. H.; Nikaitani, D.; Lien, E. J. *J. Med. Chem.* **1973**, *16*, 1207.
(21) Rekker, R. F. *The Hydrophobic Fragmental Constant*; Elsevier: Amsterdam, 1977.
(22) Hansch, C.; Rockwell, S. D.; Jow, P. Y. C.; Leo, A.; Steller, E. E. *J. Med. Chem.* **1977**, *20*, 304.
(23) We thank Drs. J. J. Morris and P. J. Taylor, I.C.I. Pharmaceuticals Division, Alderley Park, Macclesfield, Cheshire, SK10 4TG, U.K., for supplying hydrogen bonding parameter data.

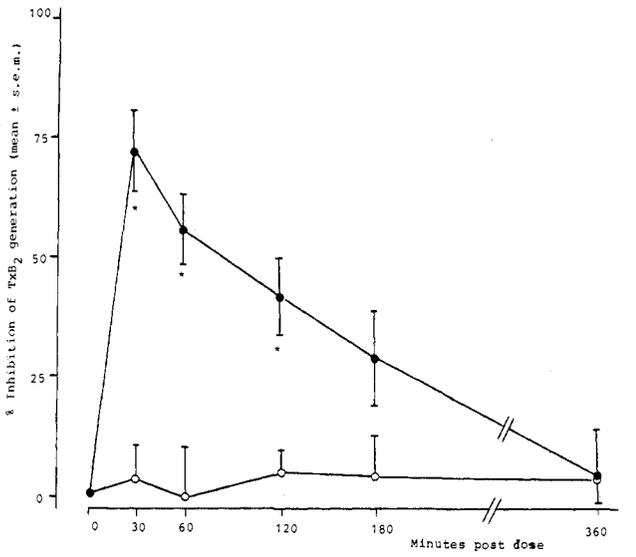

Figure 1. Effect of intravenously administered compound **5d** on collagen-induced formation of TxB_2 in rabbit citrated whole blood ex vivo. The compound (10 mg kg^{-1}; ●) and vehicle alone (acidified buffer, pH 6.0; ○) were administered to separate groups of male NZW rabbits by bolus intravenous injection ($n = 5$, each treatment). Citrated blood samples were obtained for estimation of ex vivo TxB_2 formation prior to and at 0.5, 1.0, 2.0, 3.0, and 6.0 h after dosing. Results are expressed as inhibition of ex vivo TxB_2 formation (mean % ± standard error of the mean), where (*) = $p < 0.05$ vs. vehicle controls (Student's t test).

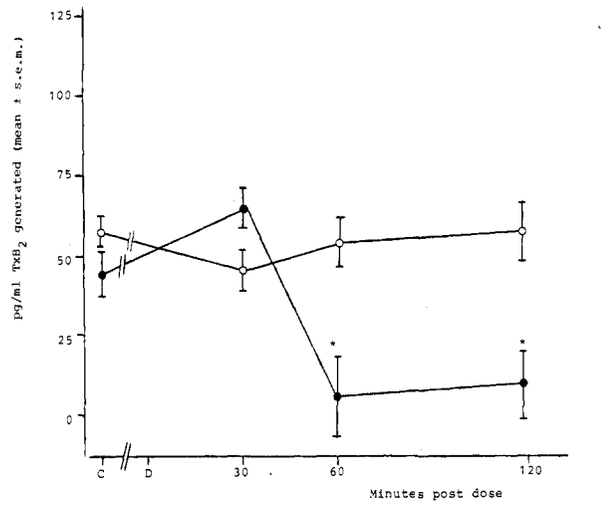

Figure 2. Effect of orally administered compound **5d** on collagen-induced formation of TxB_2 in rabbit citrated whole blood ex vivo. The compound (100 mg kg^{-1}; ●) and vehicle alone (○) were administered to separate groups of male NZW rabbits ($n = 5$ in each treatment group). Citrated blood samples were obtained for estimation of ex vivo TxB_2 formation prior to (C) and at 0.5, 1.0, and 2.0 h after dosing (D). Results are expressed as plasma TxB_2 generated (mean pg mL^{-1} ± standard error of the mean), where (*) = $p < 0.05$ vs. vehicle controls (Student's t test).

following an intravenously administered dose (estimated pharmacodynamic $t_{1/2}$ = 1.8 h) and was only evident orally at a high dose level (100 mg kg^{-1}). Likewise, the esters **5c** and **5g** also had a short duration of action following intravenous dosing (10 mg kg^{-1}).

In view of the short duration of action of the esters, the dimethylamide derivative **5p** was also tested. However, after intravenous administration (10 mg kg^{-1}) no inhibition of ex vivo collagen-induced TxB_2 formation was observed at any time point (0.5, 1, 2, 3, or 6 h).

Metabolism of 5d. One minute after intravenous infusion of [^{14}C]-**5d** (4 mg kg^{-1}) into rabbits, no native **5d** was present in either plasma or red blood cells under the extraction or HPLC conditions used. All of the radioactivity monitored by using HPLC procedure I was present in the solvent front. However, when HPLC procedure II, the ion-pair reversed-phase system, was used, the radioactive material was resolved into two major peaks, designated M_1 and M_2. M_1 contained approximately 25% of the radioactivity chromatographed and coeluted with **5m** while M_2 contained approximately 45% of the radioactivity and eluted earlier than M_1, indicating that the material was more polar. The remaining radioactivity was primarily located in a number of minor peaks present between M_1 and M_2. With increasing time after infusion of **5d** there was a general shift in the HPLC profile to multiple peaks, which were of greater polarity than M_1.

The metabolite M_1 was collected by using HPLC procedure II and rechromatographed by using HPLC procedure III, comprising a conventional reversed-phase system. As in the ion-pair HPLC procedure, M_1 coeluted with **5m**, suggesting that M_1 was the deesterified acid, **5m**. Approximately 10 mg of the metabolite M_1 was collected for mass spectral analysis using solid-probe electron-impact mass spectrometry. The similarity of the spectra obtained for M_1 and **5m** strongly suggested coidentity of M_1 with **5m**.

The major metabolite of **5d**, M_2, which eluted earlier than M_1 under all of the HPLC procedures described, was also purified and collected by using the sequential HPLC procedures II and III, which had been used for M_1. No mass spectrum could be obtained for M_2 under the conditions used for M_1. Treatment of an aliquot of the purified ^{14}C-labeled M_2 with β-glucuronidase from *Helix pomatia* resulted in a change in the retention time of M_2 when rechromatographed under HPLC procedure II or III such that all radioactivity cochromatographed with both M_1 and **5m**. These results indicate that M_2 is probably the β-glucuronyl ester of **5m**/M_1 and that the initial metabolism of **5d** proceeded by deesterification followed by β-glucuronidation and excretion.

Dazoxiben (**1**), which has an elimination half-life of 1.2 h after oral administration to humans, is also primarily metabolized via β-glucuronidation.[24]

In summary, we have investigated the structure–activity relationships of a novel series of imidazole-based TxA_2 synthase inhibitors. Although the ester **5g** was among the most active compounds tested against TxB_2 generation in intact human platelets, the parent acid **5m** was more active against the microsomal enzyme. Esters of **5m** showed a parabolic relationship between lipophilicity and inhibition of TxB_2 generation in intact platelets. These results are consistent with **5m** itself having poor platelet bioavailability, with the esters behaving as prodrugs by more readily permeating the platelet membrane prior to being enzymatically deesterified. Intravenous or oral administration of the ester **5d** to rabbits only resulted in a transient inhibition of collagen-induced TxB_2 formation, and further studies indicated that this short duration of action was a result of rapid metabolism proceeding via deesterification, followed by β-glucuronidation and excretion. Attempts at replacing the carboxylic acid group in **5m** with other potential pharmacophores were unsuccessful.

Experimental Section

Melting points (uncorrected) were determined on a Reichart Thermovar melting point apparatus. ^{1}H NMR spectra were run

(24) Stopher, D. A.; Beresford, A. P.; Kinns, M.; Bowen, D. V. *Xenobiotica* 1981, *11*, 849.

at ambient temperature on a Bruker WM 250 spectrometer at 250 MHz, with Me_4Si as an internal standard. IR spectra were run on a Perkin-Elmer 197 spectrometer. Elemental analyses were performed by C. H. N. Analysis Ltd., South Wigston, Leicester LE8 2PJ, U.K., and the results are within ±0.40% of the theoretical values.

[[(4-Methoxyphenyl)methoxy]methyl]oxirane (3a). A solution of 4-methoxybenzyl alcohol (800 g, 5.8 mol) in dry THF (1200 mL) was added dropwise to a stirred suspension of NaH (280 g of a 60% dispersion in oil, 7.8 mol) in dry THF (600 mL) at −5 °C and under a gentle stream of dry nitrogen. The mixture was allowed to warm up to room temperature and stirred until hydrogen evolution ceased. The resulting slurry of the sodium alkoxide was cooled to −5 °C and treated with epibromohydrin (860 g, 6.3 mol) at a rate such that the temperature remained below 5 °C. The reaction mixture was allowed to warm gradually to room temperature, stirred for 12 h, filtered, and washed with methanol. The combined filtrate and washings were evaporated, and the crude product (250 g) was distilled to yield pure **3a**, bp 126 °C (0.2 mmHg), as a pale yellow oil: NMR ($CDCl_3$) δ 2.70 (m, 2 H), 3.20 (m, 1 H), 3.65 (m, 2 H), 3.37 (s, 3 H), 4.73 (s, 2 H), and 7.15 (q, 4 H).

Ethyl 4-[(oxiranylmethoxy)methyl]benzoate (3b) was prepared, by the above method, with ethyl 4-(hydroxymethyl)-benzoate in place of 4-methoxybenzyl alcohol, as a pale yellow oil, which was used directly in the preparation of **4b** without purification: NMR ($CDCl_3$) δ 1.39 (t, 3 H), 2.62 (dd, 1 H), 2.81 (dd, 1 H), 3.18–3.22 (m, 1 H), 3.43 (dd, 1 H), 3.82 (dd, 1 H), 4.37 (q, 2 H), 4.64 (AB q, 2 H), 7.41 and 8.03 (AB q, 4 H).

α-[[(4-Methoxyphenyl)methoxy]methyl]-1*H*-imidazole-1-ethanol (4a). A solution of **3a** (100 g, 0.515 mol) in dry THF (200 mL) was treated with imidazole (44.4 g, 0.653 mol) and heated under reflux for 16 h. The solution was filtered and evaporated to give a brown solid, which was recrystallized from 10% water–propan-1-ol to give **4a** (83 g; 61%) as a white solid: mp 100–101 °C; NMR ($CDCl_3$) δ 3.38 (ABM oct, 2 H), 3.78 (s, 3 H), 3.86–4.14 (m, 3 H), 4.44 (s, 2 H), 5.68 (br s, 1 H), 6.83 (s, 1 H), 6.88 (s, 1 H), 6.87 and 7.24 (AB q, 4 H), and 7.32 (s, 1 H); IR (Nujol) 3100 cm^{-1} (O–H). Anal. ($C_{14}H_{18}N_2O_3$) C, H, N.

Ethyl 4-[[2-hydroxy-3-(1*H*-imidazol-1-yl)propoxy]methyl]benzoate (4b) was prepared by the above method, with **3b** in place of **3a**, as a hygroscopic yellow oil: NMR ($CDCl_3$) δ 1.39 (t, 3 H), 3.46 (ABM oct, 2 H), 3.92–4.14 (m, 3 H), 4.37 (q, 2 H), 4.59 (s, 2 H), 5.36 (br s, 1 H), 6.85 (s, 1 H), 6.91 (s, 1 H), 7.36 (s, 1 H), 7.39 and 8.02 (AB q, 4 H); IR (neat) 3400 cm^{-1} (O–H). Anal. ($C_{16}H_{20}N_2O_4 \cdot 0.6H_2O$) C, H, N.

Ethyl 4-[[2-(1*H*-Imidazol-1-yl)-1-[[(4-methoxyphenyl)methoxy]methyl]ethoxy]methyl]benzoate (5d). Method A. A solution of **4a** (75 g, 0.286 mol) in dry THF (500 mL) was added dropwise to a suspension of NaH (10 g of an 80% dispersion in oil, 0.33 mol) and stirred at room temperature for 1 h. A solution of ethyl 4-(bromomethyl)benzoate[25] (85 g, 0.35 mol) in dry THF (500 mL) was then added, and the resulting mixture was stirred for 16 h. The solvent was evaporated off, and the residue was partitioned between saturated aqueous NH_4Cl (100 mL) and EtOAc (500 mL). The EtOAc layer was washed with water and dried ($MgSO_4$). The solvent was evaporated, and the crude product was purified by column chromatography (silica gel, $CHCl_3$) to give a solid (40 g), which was recrystallized from Et_2O–pentane to give **5d** (24 g, 20%) as colorless needles: mp 58–59 °C; NMR ($CDCl_3$) δ 1.40 (t, 3 H), 3.43 (ABM oct, 2 H), 3.74 (m, 1 H), 3.82 (s, 3 H), 4.12 (ABM oct, 2 H), 4.38 (q, 2 H), 4.45 (s, 2 H), 4.47 and 4.58 (AB q, 2 H), 6.89 and 7.25 (AB q, 4 H), 6.92 (s, 1 H), 7.06 (s, 1 H), 7.26 and 7.99 (AB q, 4 H), and 7.50 (s, 1 H); IR (Nujol) 1718 cm^{-1} (C=O). Anal. ($C_{24}H_{28}N_2O_5$) C, H, N.

This method was used for the preparation of compounds **5a** and **5s**, using 4-methoxybenzyl chloride and 4-(methylthio)benzyl chloride, respectively, and of compounds **5c**, **5k**, and **5l**, using the appropriate 4-(bromomethyl)benzoic acid ester. Compounds **5b** and **5v** were also prepared by this method using **4b** in place of **4a** and the appropriate benzyl halide. In most cases the crude product was purified by column chromatography (silica gel, chloroform).

(25) Titley, A. F. *J. Chem. Soc.* **1928**, 2581.

4-[[2-(1*H*-Imidazol-1-yl)-1-[[(4-methoxyphenyl)methoxy]methyl]ethoxy]methyl]benzoic Acid (5m). A solution of **5d** (12.0 g, 0.028 mol) in 10% ethanolic KOH (30 mL) was stirred at 18 °C for 24 h. The solvent was evaporated off to give a residue, which was treated with water (100 mL), acidified with AcOH to pH 5, and extracted with CH_2Cl_2. The combined extracts were dried (Na_2SO_4) and evaporated to give a residue, which was purified by column chromatography (silica gel, 10% EtOH–CH_2Cl_2) and recrystallized from Et_2O–pentane to give **5m** (8.9 g, 80%) as a colorless crystalline solid: mp 109–111 °C; NMR ($CDCl_3$) δ 3.50 (ABM oct, 2 H), 3.68–3.80 (m, 1 H), 3.81 (s, 3 H), 4.12 (ABM oct, 2 H), 4.49 (s, 2 H), 4.36 and 4.65 (AB q, 2 H), 6.91 (s, 1 H), 6.90 and 7.26 (AB q, 4 H), 7.15 (s, 1 H), 7.72 (s, 1 H), 7.12 and 8.03 (AB q, 4 H), and 9.80 (br s, 1 H); IR (Nujol) 3110 cm^{-1} (OH). Anal. ($C_{22}H_{24}N_2O_5$) C, H, N.

Phenyl 4-[[2-(1*H*-Imidazol-1-yl)-1-[[(4-methoxyphenyl)methoxy]methyl]ethoxy]methyl]benzoate (5h). Method B. A stirred solution of **5m** (17.8 g, 0.045 mol) and Et_3N (4.87 g, 0.046 mol) in CH_2Cl_2 (150 mL) at −78 °C was treated with ethyl chloroformate (4.93 g, 0.046 mol). The solution was allowed to warm up to 0 °C over 30 min, cooled to −78 °C, and then treated with a solution of phenol (4.27 g, 0.045 mol) in CH_2Cl_2 (15 mL). The reaction mixture was allowed to warm up to room temperature and stirred for a further 2 h. The solution was evaporated, and the residue was purified by column chromatography (silica gel, $CHCl_3$) to give **5h** (11.3 g, 53%) as a hygroscopic oil: NMR ($CDCl_3$) δ 3.45 (ABM oct, 2 H), 3.68–3.80 (m, 1 H), 3.81 (s, 3 H), 4.12 (ABM oct, 2 H), 4.46 (s, 2 H), 4.49 and 4.61 (AB q, 2 H), 6.90 (d, 2 H), 6.93 (s, 1 H), 7.06 (s, 1 H), 7.19–7.46 (m, 9 H), 7.51 (s, 1 H), and 8.14 (d, 2 H); IR (liquid film) 1735 cm^{-1} (C=O); mass spectrum, *m/e* 473 ($M^+ + 1$). Anal. ($C_{28}H_{28}N_2O_5 \cdot 1.5H_2O$) C, H, N.

This method was used for the preparation of compounds **5e–g**, **5i**, **5j**, and **5n–q** using the appropriate alcohol or amine.

4-[[2-(1*H*-Imidazol-1-yl)-1-[[(4-methoxyphenyl)methoxy]methyl]ethoxy]methyl]-*N*,*N*-dimethylbenzenecarbothioamide (5r). A solution of **5p** (1.59 g, 0.0375 mol) and Lawesson's reagent (2,4-bis(4-methoxyphenyl)-1,3,2,4-dithiadiphosphetane 2,4-disulfide) (0.76 g, 0.0187 mol) in benzene (20 mL) was heated under reflux for 5 h. The mixture was dissolved in EtOAc (250 mL), and the resulting solution was washed with saturated aqueous $NaHCO_3$ and dried ($MgSO_4$). The solvent was evaporated, and the crude product was purified by column chromatography (silica gel, 50% $CHCl_3$ in hexane) to give **5r** (0.80 g, 48%) as a hygroscopic oil: NMR ($CDCl_3$) δ 3.16 (s, 3 H), 3.43 (ABM oct, 2 H), 3.79 (s, 3 H), 3.68–3.80 (m, 1 H), 3.81 (s, 3 H), 4.12 (ABM oct, 2 H), 4.58 (s, 2 H), 4.50 and 4.63 (AB q, 2 H), 6.89 and 7.22 (AB q, 4 H), 6.91 (s, 1 H), 7.03 (s, 1 H), 7.08 and 7.20 (AB q, 4 H), and 7.48 (s, 1 H); IR (liquid film) 1610 cm^{-1}; mass spectrum, *m/e* 440 ($M^+ + 1$). Anal. ($C_{24}H_{29}N_3O_3S \cdot 0.6H_2O$) C, H, N.

1-[3-[(4-Methoxyphenyl)methoxy]-2-[[4-(methylsulfinyl)phenyl]methoxy]propyl]-1*H*-imidazole (5t). A solution of *m*-chloroperoxybenzoic acid (1.69 g, 0.0098 mol) in EtOAc (10 mL) was added dropwise to a stirred solution of **5s** (3.9 g, 0.0098 mol) in EtOAc (50 mL) at −50 °C over a period of 3 h. The solution was allowed to warm up to 20 °C over a period of 6 h, then washed with 10% aqueous $Na_2S_2O_3$ solution followed by saturated aqueous $NaHCO_3$, and dried ($MgSO_4$). The solvent was evaporated, and the crude product was purified by column chromatography (silica gel, 1% EtOH in $CHCl_3$) to give **5t** (1.0 g, 25%) as a hygroscopic oil: NMR ($CDCl_3$) δ 2.70 (s, 3 H), 3.45 (ABM oct, 2 H), 3.70–3.86 (m, 1 H), 3.81 (s, 3 H), 4.11 (ABM oct, 2 H), 4.46 (s, 2 H), 4.46 and 4.59 (AB q, 2 H), 6.84 and 7.25 (AB q, 4 H), 6.86 (s, 1 H), 7.08 (s, 1 H), 7.34 and 7.58 (AB q, 4 H), and 7.50 (s, 1 H); IR (liquid film) 1040 cm^{-1} (SO); mass spectrum, *m/e* 415 ($M^+ + 1$); homogeneous on reversed-phase HPLC (μBondapak C18; 0.01% sodium dihydrogen phosphate (48%), MeOH (30%), MeCN (20%), AcOH (2%)); homogeneous on TLC (silica, 10% EtOH in $CHCl_3$). No satisfactory elemental analysis could be obtained for this compound due to its hygroscopic nature.

1-[3-[(4-Methoxyphenyl)methoxy]-2-[[4-(methylsulfonyl)phenyl]methoxy]propyl]-1*H*-imidazole (5u). *m*-Chloroperoxybenzoic acid (2.86 g, 0.0165 mol) was added in portions to a stirred solution of **5s** (3.00 g, 0.0075 mol) in CH_2Cl_2 (40 mL). The mixture was stirred for 2 h, then washed with

saturated aqueous $NaHCO_3$, and dried ($MgSO_4$). The solvent was evaporated, and the crude product was purified by column chromatography (silica gel, $CHCl_3$) and recrystallized from Et_2O–pentane to give **5u** (2.3 g, 71%) as a white solid: mp 72–74 °C; NMR ($CDCl_3$) δ 3.04 (s, 3 H), 3.47 (ABM oct, 2 H), 3.70–3.85 (m, 1 H), 3.81 (s, 3 H), 4.11 (ABM oct, 2 H), 4.47 (s, 2 H), 4.46 and 4.62 (AB q, 2 H), 6.88 and 7.25 (AB q, 4 H), 6.91 (s, 1 H), 7.04 (s, 1 H), 7.49 (s, 1 H), and 7.36 and 7.87 (AB q, 4 H); IR (Nujol) 1308 cm^{-1} (SO_2). Anal. ($C_{22}H_{26}N_2O_5S$) C, H, N, S.

Pharmacological Evaluation. In Vitro Assay of Human Whole Platelet Thromboxane Synthase. Human venous blood was collected from healthy male donors, who had denied any medication during the previous 14 days. Nine volumes of blood were mixed with 1 volume of trisodium citrate (3.24%). The citrated blood was centrifuged (160*g* for 10 min) at 22 °C to obtain platelet-rich plasma (PRP). The platelets were then counted on a Coulter counter, and the platelet count was adjusted to 200 000/μL with platelet-poor plasma. The PRP was dispensed as aliquots (500 μL) into micro-Eppendorf tubes, maintained at 37 °C in a dry bath. The compounds, dissolved in either saline, EtOH, or Me_2SO, were added in duplicate to the PRP aliquots to produce final concentrations in the range of 0.1–30 μg/mL. When EtOH and Me_2SO were used as the vehicle, triplicate controls containing the same percentage of vehicle as the test compounds were made. The final concentration of organic solvent was never more than 0.1%, which in control experiments had been shown to have no effect on TxB_2 generation.

Following a 10-min incubation with test compounds or vehicle, collagen was added to a final concentration of 8 μg/mL. The tubes were then rotor-mixed for 15 s and replaced in the dry bath for a further 10 min; controls received saline instead of collagen. The incubation was terminated by ice cooling and rapid centrifugation (15000*g* for 3 min). The plasma was removed and frozen at −30 °C until assayed. Aliquots (100 μL) of the following, in phosphate, pH 6.8, buffer (50 mM) + 0.1% gelatin + thimerosal, were incubated together for 16 h at 4 °C: TxB_2 (plasma extract or standards 50–10 000 pg/mL), [^{3}H]TxB_2 (ca. 15 000 dpm), and anti-TxB_2 antiserum (0.5 μg/μL). The free and protein-bound [^{3}H]TxB_2 were separated by absorption onto activated charcoal followed by centrifugation. A 1.0-mL volume of the supernatant was added to an aqueous scintillation fluid, and the radioactivity present was counted in a liquid scintillation counter. The binding of [^{3}H]TxB_2 in the absence of added TxB_2 was ca. 55%. The least amount of TxB_2 to be detected accurately in the plasma was 50 pg/mL. Cross reactivity with other prostaglandins was less than 0.005% except PGD_2, which was 1%. Thus plasma samples were assayed to give a rough approximation of TxB_2 content. The plasma was then appropriately diluted and assayed in duplicate to give accurate values. The amount of TxB_2 generated by the collagen was calculated by subtracting mean values obtained for the saline-stimulated platelets from the mean values obtained for the collagen-stimulated platelets. Then the concentration of compound producing a 50% inhibition of the control sample TxB_2 generation (IC_{50}) was determined by computer analysis of the dose–response curves using a logit transformation of the data with subsequent linear regression treatment.

In Vitro Assay of Human Platelet Microsomal Thromboxane Synthase. PRP (10 mL) was obtained from citrated whole blood by centrifugation, as above. Platelets were spun down at 300*g* for 10 min, and the platelet pellet was resuspended in 5 mL of NaCl (0.15 M)–Tris·HCl, pH 7.4, buffer (0.15 M) containing EDTA (77 μM) (90:8:2, v/v), washed, and finally resuspended in 5 mL of NaCl (0.15 M)–Tris·HCl, pH 7.4, buffer (0.15 M) (90:10, v/v). The cells were then sonicated (2 × 1 min), and the sonicate was centrifuged at 10000*g* for 15 min. The cloudy supernatant was further centrifuged at 100000*g* for 60 min. The resulting microsomal pellet (30–40 μg of protein) was suspended in 100 μL of Tris·HCl, pH 7.4, buffer (50 mM) at 25 °C and was preincubated with vehicle or drug (2 μL in acidified buffer) for 5 min prior to initiation of the reaction by addition of PGH_2 substrate (final concentration 15 μM). After a 3-min incubation period, the reaction was terminated by the addition of HCl (5 μL of 1 M) and all samples were then neutralized by a further addition of Tris-base (5 μL of 1 M). TxB_2 formation was measured by radioimmunoassay, and the concentration of compound producing a 50% inhibition of the vehicle sample TxB_2 generation (IC_{50}) was determined by computer analysis of the dose–response curves.

In Vitro Assay of Human Whole Platelet Prostaglandin E_2 Formation. The methods employed for preparation of human PRP and the technique used for incubation of PRP samples in the presence of collagen (with or without drug) were identical with those described for measuring whole human platelet TxA_2 synthase activity (above). Plasma levels of PGE_2 were also determined by an essentially similar radioimmunoassay procedure using commercially available [^{3}H]PGE_2 and a specific rabbit antibody to PGE_2 (Sigma).

In Vitro Assay of Bovine Fetal Heart Endothelial Cell Prostacyclin Formation. Bovine fetal heart endothelial cells were grown to confluence in culture, trypsinized, and suspended in Eagle's medium 199, aliquots were plated out into a 24 × 1.0 mL multiwell microtiter plate, and the cells were allowed 48 h to "carpet down". On the day of the experiment, dilutions of drug (0.1–100.0 μM) or vehicle equivalent (Me_2SO to a maximum volume of 1 μL/well) were added to individual wells in each plate and mixed by gentle agitation of the plate. After a 3-min preincubation period at 37 °C in the presence of drug, arachidonic acid (10 μM; sodium salt dissolved in 100 mM Tris buffer, pH 8.0) was added to each well. The incubation was terminated after a further 10 min by removal of the cell supernatant, immediate centrifugation (2 min at 10000*g*), and freezing of samples until assay. PGI_2 formation was estimated in diluted (1:10) aliquots of cell supernatant by radioimmunoassay for immunological equivalents of the stable breakdown product 6-keto $PGF_{1\alpha}$ essentially as described for TxB_2 (above), using isotope and a specific antibody supplied by New England Nuclear.

Ex Vivo Evaluation of Compounds vs. Collagen Induced Whole Blood Thromboxane B_2 Formation. (a) Intravenous Efficacy. Rabbits (NZW males, 3–3.5 kg) were anesthetized with pentabarbitone sodium (65 mg/kg) by intraperitoneal injection. The trachea was cannulated to ensure a free airway, and an indwelling cannula was placed in the left external carotid artery for withdrawal of blood samples. Drugs were administered in acidified saline (pH 6) by intravenous injection via a lateral ear vein.

(b) Oral Efficacy. Conscious rabbits (as above) were dosed orally by gavage with drug or vehicle alone (a formulation of polyethylene glycol 400 (10%) and (carboxymethyl)cellulose (90%, v/v)). Blood samples were obtained from the central ear artery at the time points specified in the text.

(c) Incubation Technique. Blood samples obtained in both intravenous and oral studies were anticoagulated with 3.28% trisodium citrate (9:1, v/v). Aliquots (0.5 mL) of citrated whole blood were stirred at 1000 rpm and equilibrated at 37 °C for 2 min prior to addition of collagen (10 μg/mL) or buffer as control. The incubation was continued for 5 min after addition of collagen, at which time formation of TxB_2 reached a plateau, and was terminated by addition of indomethacin (28 μM) and chilling on ice. Plasma samples were obtained by centrifugation (10000*g* for 2 min) and frozen at −30 °C until radioimmunoassay for TxB_2 as described above.

Metabolic Studies. Estimation of in Vivo Half-Life of 5d and Identification of Metabolites. Rabbits (8 NZW males, 3–3.5 kg) anesthetized initially with pentabarbitone (30 mg/kg, ip) were maintained with halothane while being respirated with intermittent positive pressure ventilation. The animals were infused through a jugular cannula with 5 μCi of [2-^{14}C]-imidazole-labeled **5d** that had been diluted with cold **5d** to produce a dose of 4 mg/kg. Serial blood samples were removed from a carotid cannula at 1, 5, 10, 20, 30, 60, and 120 min after infusion. Blood samples were separated into plasma and red blood cell fractions by centrifugation (1000*g* × 10 min) and subjected to extraction and HPLC procedures.

Extraction Procedures. Standardized extraction procedures were developed to separate **5d** or **5m** from plasma and red blood cells in a quantitative and reproducible manner.

Extraction Procedure I. Aqueous samples of **5d** (0.25 mL) were adjusted to pH 9.0 with NaOH (1 M) and extracted with Et_2O (3 × 10 mL). The combined extracts were evaporated under N_2 and reconstituted in an appropriate HPLC mobile phase. Extraction efficiency was 90%.

Extraction Procedure II. Aqueous samples of **5m** (0.25 mL) were adjusted to pH 2.0 with HCl (1 M), extracted with Et_2O,

and reconstituted as described for **5d**. Extraction efficiency was greater than 80%.

Separation Procedures. Three HPLC procedures were developed, one for the isolation and identification of **5d** and two for **5m**.

Procedure I: HPLC Separation of 5d. Stationary phase: Ultrasphere ODS precolumn (4.6 mm × 45 mm) with a 5-μm Ultrasphere ODS analytical column (4.6 mm × 250 mm). Mobile phase: 60% CH_3CN, 40% sodium phosphate buffer (0.025 M), pH 7.2. Flow rate: 1 mL/min. Temperature: ambient. Either detection was spectrophotometric using a fixed-wavelength detector with a 229-nm filter (cadmium lamp) or fractions were collected for subsequent scintillation counting. The retention time for **5d** was 10.4 min.

Procedure II: HPLC Separation of 5m Using Reversed-Phase Ion-Pair Chromatography. Stationary phase: Ultrasphere ion-pair precolumn (4.6 mm × 45 mm) with a 5-μm Ultrasphere ion-pair analytical column (4.6 mm × 250 mm). Mobile phase: 55% MeOH, 22.5% tetrabutylammonium hydroxide (0.025 M), 22.5% potassium phosphate, pH 8.0, buffer (0.02 M). Flow rate: 1.2 mL/min. Temperature: 35 °C. Either detection was spectrophotometric using a fixed-wavelength detector with a 229-nm filter (cadmium lamp) or fractions were collected for subsequent scintillation counting. The retention time for **5m** was 28 min.

Procedure III: HPLC Separation of 5m Using Reversed-Phase Chromatography. Stationary phase: Ultrasphere ODS precolumn (4.6 mm × 45 mm) with a 5-μm ultrasphere ODS analytical column (4.6 mm × 250 mm). Mobile phase: 35% MeOH, 65% potassium phosphate, pH 5.3, buffer (20 mM). Flow rate: 1 mL/min. Temperature: ambient. Detection was as described above. The retention time for **5m** was 24.5 min.

Mass Spectral Analysis of M_1. A sample of metabolite M_1 (50 mg) was purified under HPLC conditions **III** by collecting fractions eluting from the HPLC column that coeluted with the radioactive peak for M_1. The material collected was evaporated to dryness under N_2. Mass spectra were obtained by using a Finnigan 4000 series quadrupole mass spectrometer. Solid-probe electron-impact ionization spectra of both **5m** and M_1 were obtained.

β-Glucuronidase Deconjugation and Mass Spectral Analysis of M_2. The purified metabolite (0.1 mg) M_2 was incubated in a volume of 2 mL in potassium phosphate, pH 5.0, buffer (0.2 M) containing 1000 units of β-glucuronidase derived from *Helix pomatia*. The incubation was maintained at 37 °C for 6 h prior to extraction and chromatography under the conditions previously described. Under the conditions of the incubation any sulfatase activity present in the β-glucuronidase would have been inhibited by the high concentration of phosphate present. The deconjugated product was subjected to mass spectral analysis as above.

Acknowledgment. We thank R. L. Dyer and M. D. Gray for the synthesis of [^{14}C]-**5d** and R. Brownsill and J. Firth for mass spectral analysis. We also express our appreciation to J. Brand for the preparation of the manuscript.

Registry No. **3a**, 108836-41-5; **3b**, 108836-42-6; **4a**, 108836-43-7; **4b**, 108836-44-8; **5a**, 108836-45-9; **5b**, 108836-45-9; **5c**, 108836-46-0; **5d**, 108836-47-1; **5e**, 108836-48-2; **5f**, 108836-49-3; **5g**, 108836-50-6; **5h**, 108836-51-7; **5i**, 108836-52-8; **5j**, 108836-53-9; **5k**, 108836-54-0; **5l**, 108836-55-1; **5m**, 108836-56-2; **5n**, 108836-57-3; **5o**, 108836-58-4; **5p**, 108836-59-5; **5q**, 108836-60-8; **5r**, 108836-61-9; **5s**, 108836-62-0; **5t**, 108836-63-1; **5u**, 108836-64-2; **5v**, 108836-65-3; 4-methoxybenzyl alcohol, 105-13-5; epibromohydrin, 3132-64-7; ethyl 4-(hydroxymethyl)benzoate, 15852-63-8; imidazole, 288-32-4; ethyl (4-(bromomethyl)benzoate, 26496-94-6; 4-(methoxybenzyl chloride, 824-94-2; 4-(methylthio)benzyl chloride, 874-87-3; methyl 4-(bromomethyl)benzoate, 2417-72-3; ethyl 3-(bromomethyl)-benzoate, 62290-17-9; 5-(bromomethyl)-1,3-dihydroisobenzofuran-1-one, 63113-10-0.

Novel Inhibitors of Rat Lens Aldose Reductase: *N*-[[(Substituted amino)phenyl]sulfonyl]glycines

Charles A. Mayfield and Jack DeRuiter*

Division of Medicinal Chemistry, Department of Pharmacal Sciences, School of Pharmacy, Auburn University, Auburn University, Alabama 36849. *Received February 9, 1987*

A number of *N*-[[(substituted amino)phenyl]sulfonyl]glycines **3a–n** were synthesized as analogues of the simple (phenylsulfonyl)glycines **1a–c** with increased lipophilic character and therefore greater aldose reductase inhibitory potential. The 2-benzoylamino derivative **3c** was found to be less potent than the corresponding amine **1c** as an inhibitor of rat lens aldose reductase, but both the 3- and 4-benzoylamino analogues, **3b** and **3a**, are substantially more potent than their amines **1b** and **1a**; compound **3a** is the most effective inhibitor of this series, with an IC_{50} of 0.41 μM. The 4-benzoylamino derivative **3a** is also significantly more active than the 4-acetylamino analogue **3d** and the 4-benzylamino (**3e**) and 4-dimethylamino (**3f**) derivatives, suggesting that both the additional carbonyl moiety and aromatic ring present in this compound may bind to complementary sites present on the enzyme. Furthermore, structure–activity studies reveal that increasing the number of atoms between the carbonyl and aromatic moieties of **3a** results in a decrease in inhibitory activity. Kinetic studies demonstrate that **3a**, like other known inhibitors of aldose reductase, functions as an uncompetitive inhibitor with respect to the substrate and therefore may interact at the proposed common inhibitor binding site of this enzyme.

As described earlier in considerable detail,[1–3] there is mounting evidence linking the conversion of glucose to sorbitol by aldose reductase in ocular and nerve tissues to the development of several chronic diabetic pathologies including cataracts, retinopathy, and peripheral neuropathy.[1–3] Thus, one approach currently investigated to prevent or at least delay the onset of diabetic pathologies has involved the development of inhibitors of the enzyme aldose reductase.[3–7] In a previous paper, we described the

(1) Dvornik, D.; Simard-Duquesne, N.; Krami, M.; Sestanj, K.; Gabbay, K. H.; Varma, S. D.; Merola, L. O. *Science (Washington, D.C.)* **1973**, *182*, 1146.
(2) Lipinski, C. A.; Hutson, N. J. *Annu. Rep. Med. Chem.* **1984**, *19*, 169.
(3) Kador, P. F.; Kinoshita, J. H.; Sharpless, N. E. *J. Med. Chem.* **1985**, *28*, 841.
(4) DeRuiter, J.; Brubaker, A. N.; Millen, J.; Riley, T. N. *J. Med. Chem.* **1986**, *29*, 627.
(5) Brubaker, A. N.; DeRuiter, J.; Whitmer, W. L. *J. Med. Chem.* **1986**, *29*, 1094.
(6) DeRuiter, J.; Brubaker, A. N.; Whitmer, W. L.; Stein, J. L. *J. Med. Chem.* **1986**, *29*, 2024.
(7) DeRuiter, J.; Brubaker, A. N.; Garner, M. A.; Barksdale, J. M.; Mayfield, C. A. *J. Pharm. Sci.* **1987**, *76*, 149.

0022-2623/87/1830-1595$01.50/0